The behavior of Aluminium Carbon/Epoxy fibre metal laminate under quasi-static loading

N K Romli[1*], M R M Rejab[1], D Bachtiar[1], J Siregar[1], M F Rani[2], W S W Harun[1], Salwani Mohd Salleh[1] and M N M Merzuki[1]

[1]Structural Materials & Degradation Focus Group, Faculty of Mechanical Engineering, Universiti Malaysia Pahang, 26600 Pekan, Pahang, Malaysia
[2]Faculty of Engineering, DRB-Hicom University of Automotive Malaysia, 26607 Pekan, Pahang, Malaysia

[*]Corresponding author email: khaleedaromli@gmail.com

Abstract. One of major concerns that related to the flight safety is impact of birds. To minimize the risks, there is need to increase the impact resistance of aircraft by developing a new material and has the good structural design of aircraft structures. The hybrid laminates are potential candidate material to be applied for the aircraft structures susceptible to bird strikes. The fibre metal laminate was fabricated by a compression moulding technique. The carbon fibre and aluminium alloy 2024-0 was laminated by using thermoset epoxy. A compression moulding technique was used for the FML fabrication. The aluminium sheet metal has been roughening by a metal sanding method which to improve the bonding between the fibre and metal layer. The main objective of this paper is to determine the failure response of the laminate under five variations of the crosshead displacement in the quasi-static loading. The FML was modelled and analysed by using Explicit solver. Based on the experimental data of the quasi-static test, the result of 1 mm/min was 11.85 kN and higher than 5, 10, 50 and 100 mm/min which because of the aluminium ductility during the impact loading response. The numerical simulations were generally in good agreement with the experimental measurements.

1. Introduction

A fibre metal laminate (FML) or also known as a hybrid laminate contains metal layers and composite materials [1-5]. The fibre metal laminate can be applied to many applications because of the fibre metal laminate can withstand to the impacts, loadings and harsh environments for a long period. The combination of the metal layers and composite fibres produce superior characteristics such as fatigue and fracture. Besides that, the substitutions of both materials are to reduce the weight of the aircraft structures and saving in oil consumption [5-11]. The Glare and Arall are members of fibre metal laminates. The fibre metal laminate started and applied in military application after the Second World War [12-23]. From the positive feedbacks of the application, the fibre metal laminate began the application widely in aircraft structures such as fuselage and wings [24, 25]. The example of the application is in the Airbus A380 due

to the improvement in fatigue, resistance to corrosion and impact and weight reduced nearly 794 kg [26-29]. The other organisations such as NASA, Bombardier and EMBRAER interested with the substitution of the aluminium in a fibre metal laminate. The high strength and stiffness are a good combination and resulted in great performance in space applications [12].

An autoclave commonly used in manufacturing o fibre metal laminates or curing process at a high pressure. The curing temperature should be maintained as well. The FMLs need to be processed up to 120˚C as to avoid damage on the aluminium alloy 2024-T3. The temperature will allow an excess of resin flow out and reduced its viscosity. The pressure will press and consolidate the plies then suppress the voids [23, 30-36]. The shear thickening fluid is a combination of hard metal oxide particles which suspended in the liquid polymer. The STF can lead the laminates to improve resistance from ballistic impact damage [37].

The debonding process between a sheet metal layer and composite fibre layer, delamination of the composite layers, fracture due to a plasticity behaviour of a metal are commonly happened to a fibre metal laminate structure which because of the impact of a load and depended on the layup configurations [6, 10, 11, 38-40]. The process of curing by using an autoclave will take long hours of processing and required intensive of labour cost for the whole production [9, 41].

The purpose of this paper to investigate the failure behaviour through an experiment of quasi-static impact test and predict the failure behaviour by using Abaqus/Explicit.

2. Experimental work

The behaviour of a fibre metal laminate was studied based on the aluminium alloy 2024-0 sheets and unidirectional carbon fibre prepreg. The prepreg fibre was bonded with the two sheet metal layers. The surface of the aluminium alloy was treated through a metal sanding. The grit size of sand paper is 100. The purpose of the metal sanding is for surface roughness. The surface roughness will increase the bonding strength between the sheet metal and glass fibre. The layup configuration of the FML is 2/1. The size and thickness of the FML are 150 mm x 150 mm and 2.15 – 2.52 mm. The FML was fabricated by a compression moulding technique. The glass fibre and aluminium alloy sheet metal alloy laminated by using the thermoset epoxy. A pressure was applied by placing a moderated load on it and cured in at room temperature for 24 hours. The shape and size of the indenter are hemisphere and 12.7 mm. The indenter fabricated through a machining process which is a CNC machine. The coolant was applied during the machining process as to reduce the cutting force temperature of the machining process.

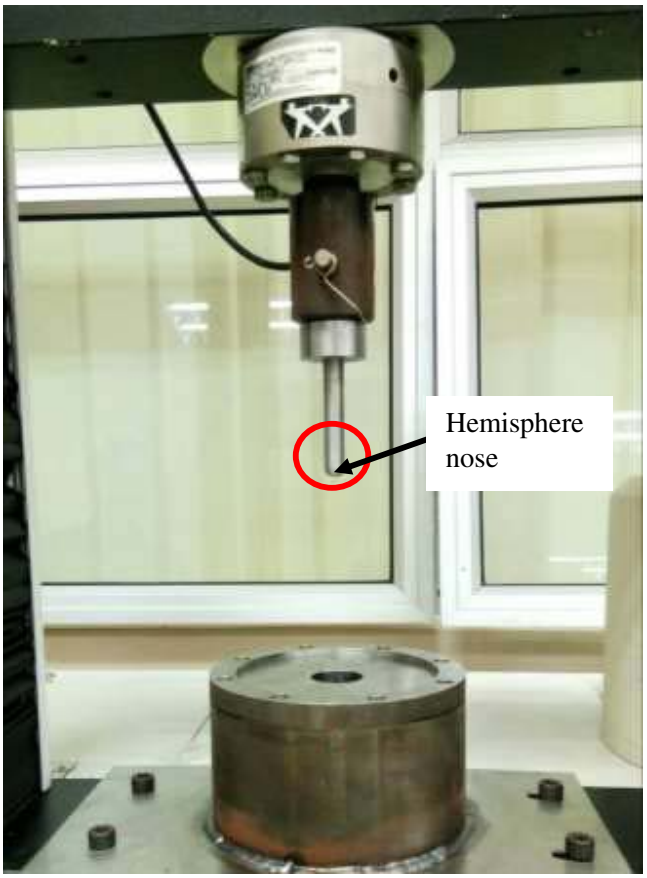

Figure 1. The setup for quasi-static test.

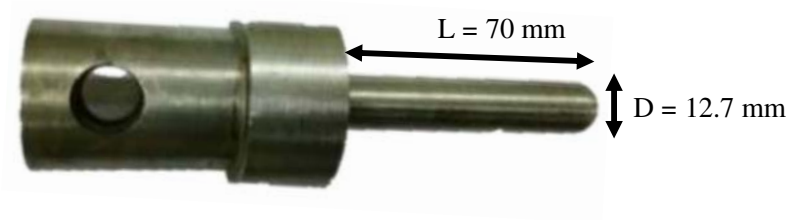

Figure 2. Hemispherical indenter.

3. Computational model

The alternative way to predict the experimental result is by using numerical analysis. Study of numerical analysis on fibre metal laminate became crucial as to know impact behaviour of it. The process of simulation could be done by adding the properties material used such as Young's modulus, Poisson's ratio, the density of the materials and so on. The simulation process required reasonable numbers of structural tests for a validation process. The previous researchers have combined two theories of failure criteria and plasticity as to simulate the degradation behaviour of the plate and study the behaviour of the nonlinear numerical model. The damage of an impact was controlled by degradation of the stiffness and fracture was because of energy releases which aimed to delamination growth. The simulation of

deformation process of 3D FE model involved sensitivity of strain-rate and large changes in transverse compression. The damaged of composite plies cannot be used directly in Abaqus [42].

The Abaqus/Explicit was used to develop a numerical simulation of the FML under the low-velocity impact. The FML consisted with two different of constituent materials; 2024-0 and unidirectional prepreg carbon fibre. The failure of the FML depended on the ductility of the materials.

3.1. Modelling of the 2024-0 by using Isotropic

The aluminium alloy 2024-0 was modelled by using an isotropic elastoplasticity to predict elastic and plastic behaviour either as a rate-dependent or rate dependent model and it has a simple form.

3.1.1 Elasticity

A model of isotropic linear elasticity was generated for the elastic respond for a material in a numerical analysis. The material that performed the linear elastic behavior, the total stress defined through this an equation:

$$\sigma = D^{el}\varepsilon^{el} \tag{1}$$

Where σ the total stress, D^{el} is the fourth order of an elasticity tensor and ε^{el} is the total elastic strain. From the Equation (1) the stress-strain relationship of isotropic linear elasticity strain:

$$\begin{bmatrix}\sigma_{11}\\ \sigma_{22}\\ \sigma_{33}\\ \sigma_{12}\\ \sigma_{13}\\ \sigma_{23}\end{bmatrix} = \frac{E}{(1+\upsilon)(1-2\upsilon)}\begin{bmatrix} 1-\upsilon & \upsilon & \upsilon & 0 & 0 & 0\\ \upsilon & 1-\upsilon & \upsilon & 0 & 0 & 0\\ \upsilon & \upsilon & 1-\upsilon & 0 & 0 & 0\\ 0 & 0 & 0 & \frac{(1-2\upsilon)}{2} & 0 & 0\\ 0 & 0 & 0 & 0 & \frac{(1-2\upsilon)}{2} & 0\\ 0 & 0 & 0 & 0 & 0 & \frac{(1-2\upsilon)}{2}\end{bmatrix}\begin{bmatrix}\varepsilon_{11}\\ \varepsilon_{22}\\ \varepsilon_{33}\\ \varepsilon_{12}\\ \varepsilon_{13}\\ \varepsilon_{23}\end{bmatrix} \tag{2}$$

The symbol of E is a Young's modulus and υ is a Poisson's ration. These have been defined in the equation above. The inverse relationship defined as an equation below:

$$\begin{bmatrix}\varepsilon_{11}\\ \varepsilon_{22}\\ \varepsilon_{33}\\ \gamma_{12}\\ \gamma_{13}\\ \gamma_{23}\end{bmatrix} = \begin{bmatrix} \frac{1}{E} & \frac{-\upsilon}{E} & \frac{-\upsilon}{E} & 0 & 0 & 0\\ \frac{-\upsilon}{E} & \frac{1}{E} & \frac{-\upsilon}{E} & 0 & 0 & 0\\ \frac{-\upsilon}{E} & \frac{-\upsilon}{E} & \frac{1}{E} & 0 & 0 & 0\\ 0 & 0 & 0 & \frac{1}{G} & 0 & 0\\ 0 & 0 & 0 & 0 & \frac{1}{G} & 0\\ 0 & 0 & 0 & 0 & 0 & \frac{1}{G}\end{bmatrix}\begin{bmatrix}\sigma_{11}\\ \sigma_{22}\\ \sigma_{33}\\ \sigma_{12}\\ \sigma_{13}\\ \sigma_{23}\end{bmatrix} \tag{3}$$

$$G = \frac{E}{2(1+\upsilon)} \tag{4}$$

G is a shear modulus. The elastic material in the properties of aluminium 2024-0 was used in the numerical modelling. The properties were taken from experimental results. The value of Young's modulus, $E = 70.6$ GPa and the Poisson's ratio is $\upsilon = 0.3$.

3.1.2 Yielding

An isotropic yielding is applied to a von Mises yield surface. The surface is assumed that yielding of a metal is independent where the observation was confirmed by experimental works. The metal was applied under a positive pressure stress. When the metal applied in that kind of situation which high-pressure stress, it may be inaccurate because voids can nucleate and grow in the metal.

3.1.3 Plasticity

Beyond the yield point is a permanent deformation or called as the plastic behavior of the aluminium. The plastic behavior is defined in an isotropic hardening. To describe the isotropic hardening, the yield stress, σ^0 which given in a plastic strain tabular function. The interpolation of the yield stress at any plastic strain rate can be done from the table of data. The data will remain constant when it reached to the last value that has been given in the table. Decomposition of the total increment of strain defined as below:

$$d\varepsilon = d\varepsilon^{el} + de^{pl} \tag{5}$$

For rate-dependent of material the relationship of the equivalent plastic strain rate, $\bar{\varepsilon}^{pl}$ followed by the uniaxial flow rate definition as:

$$\bar{\varepsilon}^{pl} = \varphi\left(q, \bar{\varepsilon}^{pl}, \theta_r\right) \tag{6}$$

φ known as a function, q is the von Mises equivalent stress, $\bar{\varepsilon}^{pl}$ is an equivalent of the plastic strain and θ_r is the temperature.

3.1.4 Failure Criteria

The development of damage and failure of ductile material are used in Abaqus/Explicit to model the damage behavior of the aluminium. *SHEAR FAILURE and *TENSILE FAILURE or a combination of both are two material failure models will offer in the Abaqus to account the damage and failure in a ductile metal. To calculate the failure, shear and tensile failure models can use an equivalent of the plastic strain and hydrostatic cut-off stress respectively. If the failed meshes removed from the meshes it may for both failure models.

3.1.5 Damage for Ductile Metals

There is two mechanisms for the ductile metals will be used in this study; ductile damage and shear damage models. The ductile fracture or ductile damage is an initial criterion for predicting the onset damage which due to nucleation, growth and the voids. This model will active when the following condition is satisfied:

$$\omega_D = \int \frac{d\bar{\varepsilon}^{pl}}{\bar{\varepsilon}_D{}^{pl}\left(\eta, \bar{\varepsilon}^{pl}\right)} = 1 \tag{7}$$

ω_D is a state variable that increases monotonically with plastic deformation. The model is assumed that the equivalent plastic strain at the onset of damage, $\bar{\varepsilon}_D{}^{pl}$ is a function of triaxiality, $\eta = -p/q$, and the equivalent of plastic strain, $\bar{\varepsilon}^{pl}$. Note that *p* is the pressure stress and *q* is the Mises equivalent stress.

The shear damage model is a fracture which due to shear band localisation in the ductile metals. The model will active when the following condition is satisfied:

$$\omega_s = \int \frac{d\bar{\varepsilon}^{pl}}{\bar{\varepsilon}_s{}^{pl}\left(\theta_s, \bar{\varepsilon}^{pl}\right)} = 1 \tag{8}$$

ω_s is a state variable that increases monotonically with plastic deformation and is relative to the incremental change in equivalent plastic strain, $\bar{\varepsilon}^{pl}$. The model is assumed that the equivalent plastic strain at the onset of damage, $\bar{\varepsilon}_s{}^{pl}$ is a function of the shear stress ratio, $\theta_s = (q + k_s p)/\tau_{\max}$ and the equivalent plastic strain rate, $\bar{\varepsilon}^{pl}$. Note that $\tau_{\max}$ is the maximum shear stress k_s is a material parameter (k_s = 0.3 for the aluminium alloy) [43].

3.2 Modelling of the composite by Hashin damage criterion.

The modelling for the composite material, woven fabric carbon fibre reinforced plastic was followed based on the table below:

Table 1: Properties of woven CFRP

Property	Symbol	Value
Young's modulus in longitudinal direction	E_{11} (GPa)	48
Young's modulus in transverse direction	E_{22} (GPa)	48
Young's modulus in thickness direction	E_{33} (GPa)	1
In-plane shear modulus	G_{12} (GPa)	9
Through-thickness shear modulus	G_{13}, G_{23} (GPa)	9
In-plane Poisson's ratio	υ_{12}	0.1
Through-thickness Poisson's ratio	$\upsilon_{13}, \upsilon_{23}$	0.1
Longitudinal tensile strength	X_T (MPa)	550
Longitudinal compressive strength	X_C (MPa)	150
Transverse tensile strength	Y_T (MPa)	550
Transverse compressive strength	Y_C (MPa)	150
Transverse shear strength	S_T (MPa)	120
Longitudinal shear strength	S_L (MPa)	120

The Hashin damage criterion based on works of Hashin and Rotem and Hashin [44, 45]. This criterion is unlike other criteria like Tsai-Hill and Tsai-Wu[46, 47]. Those criteria purposed an equation to predict damage initiation. The Hashin damage presents four failure modes with four corresponding indexes (a) breakage of fibre from the tension $\left(F_f{}^t\right)$, (b) buckle of fibre from the compression $\left(F_f{}^c\right)$, (c) crack of the matrix from the tension $\left(F_m{}^t\right)$ and (d) crush of the matrix from the compression $\left(F_m{}^c\right)$. There is four equation that applied to those failure modes respectively:

$$\left(F_f{}^t\right)=\left(\frac{\sigma_{11}}{S_{t1}}\right)^2+\alpha\left(\frac{\sigma_{12}}{S_{12}}\right)^2\le 1.0 and \sigma_{11}\ge 0 \tag{9}$$

$$\left(F_f{}^c\right)=\left(\frac{\sigma_{11}}{S_{c1}}\right)^2\le 1.0 and \sigma_{11}<0 \tag{10}$$

$$\left(F_m{}^t\right)=\left(\frac{\sigma_{22}}{2S_{s23}}\right)^2+\alpha\left(\frac{\sigma_{c2}}{2S_{s23}}\right)^2\le 1.0 and \sigma_{22}\ge 0 \tag{11}$$

$$\left(F_m{}^c\right)=\left(\frac{\sigma_{22}}{2S_{s23}}\right)^2+\left[\left(\frac{S_{c2}}{2S_{s23}}\right)^2-1\right]\frac{\sigma_{22}}{S_{c2}}+\left(\frac{\sigma_{12}}{S_{12}}\right)^2\le 1.0 and \sigma_{22}<0 \tag{12}$$

σ_{11}, σ_{22} and σ_{12} are applied stresses while α is a coefficient of the shear stress σ_{12} which contributed in fibre breakage by a tension criterion. In the Abaqus, the criterion of Hashin could be implemented in a conjunction with a damage evolution law. The law based on a specification of four fracture energyvalues G_f. The values corresponded to the material degradation in each mode. The values constituent in an implementation of the Hashin-based and analysed with the damage evolution in the Abaqus. The damage variable for fibres d_f, matrix d_m and shear d_s were assessed by this expression [48]:

$$d=\frac{\delta^f{}_{eq}\left(\delta_{eq}-\delta^0{}_{eq}\right)}{\delta_{eq}\left(\delta^f{}_{eq}-\delta^0{}_{eq}\right)} \tag{13}$$

$\delta^f{}_{eq}$ is an equivalent of a displacement in an FE when the stress reached to zero in a stress-displacement while $\delta^0{}_{eq}$ is an equivalent of a displacement when the damage initiated. δ_{eq} is an equivalent of a displacement in FE for the given applied strain [48].

4. Results and Discussion

The damaged area of the laminate is depended on a crosshead displacement of the quasi-static loading. The crosshead displacement and the constituent materials, the 2024-0 aluminium alloy and carbon fibre reinforced polymer were in the present case. The prior to testing, the type of resin used and metal sanding were investigated. The thermoset epoxy was used as a matrix to laminate the carbon fibre with the aluminium alloy. The sandpaper with grit 80 was applied on the aluminium alloy as to increase the bonding between the sheet metal and matrix. From the graph, it showed that the trending of failure on the fibre metal laminate became decreased when the crosshead displacement was increased from 1 mm/min to 100 mm/min.

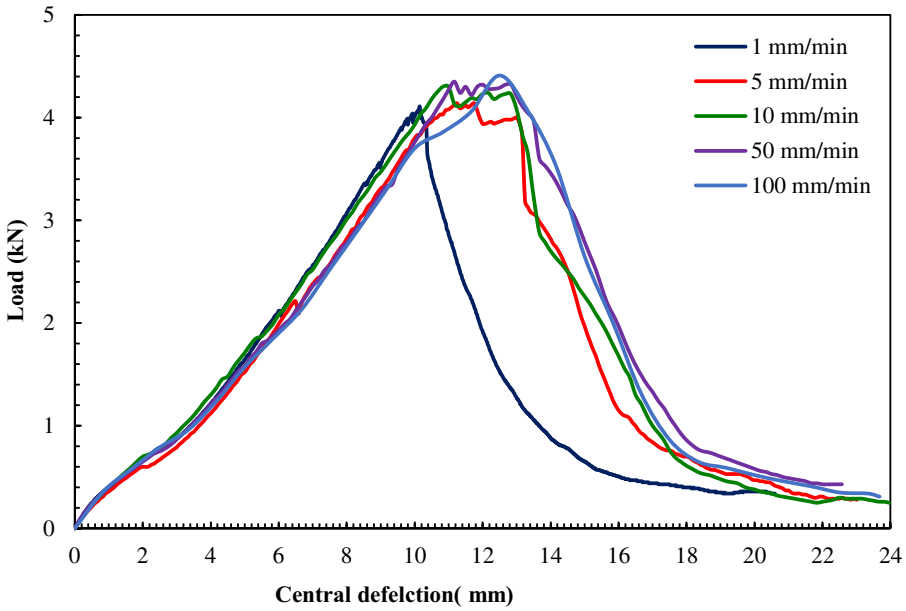

Figure 3. Graph of load against central deflection in Aluminium/CFRP FML

The failure process of the quasi-static indentation on the FML was investigated by examining the front surface and rear-surface of the impact damaged samples. The initial fracture onto the 2/1 FML by 1 mm/min crosshead displacement. The experiment was handle by using Instron 3369 Universal Testing Machine. The 1 mm/min impact shown in a Figure 4a. The damaged area has been taken through an indentation stage by the indenter at a top surface of the aluminium alloy. At the second stage, there was a localize crack on the matrix. The failure on the matrix because of the preparation of layup process. The laminate start to bend because of the maximum load that acted on it and the laminate has a maximum bending. After that, there was a fibre breakage because of the maximum bending of the loading and the stiffness of the fibre. Then, there was an indentation on the bottom ply, aluminium alloy. The perforation on the laminate happened at the third stage of failure. The passage of the indenter through the target and produce a clean hole with a diameter that similar to the indenter. From the graph, the perforation involved a local ductility.

The higher crosshead displacement resulted in a decrease of composite structure degradation. Besides that, there was a number of transverse cracks which increases the delamination of the laminate especially at the middle area of the specimen. The matrix crack also caused delamination of the laminate. When the testing was carried out with the lowest crosshead displacement of quasi-static loading it resulted in an extensive delamination at the middle part and bottom ply. When the crosshead displacement increased, the deformation on the fibre metal laminate happened at the same time. The matrix of the laminate damaged caused by impact and the connection between matrix-fibre became degradation. The epoxy resin is brittle and has low resistance to the crack propagation. The crack happened at a high transverse shearing stress which connected with the contact force. The bending crack occurred easily if the volume of the matrix is higher than the volume of the fibre.

In the experimental works, the range of crosshead displacement 1-100 mm/min involved delamination layer, failure of the fibre, plastic deformation and cracking of the aluminium layer. The energy lost

defined as $1-\eta$ will be decreasing when the impact crosshead displacement was increased. η is energy absorption factor. The lost energy would constituent the energy which used to rebound the impactor. Besides that, the energy also used as to overcome the friction from the indenter and during the impact, a sound would be produced. The sound signed for the failure of the fibre and cracking of the aluminium alloy. The deformation behavior of the top surface have been shown in the **Fig 4** respectively. The increasing of impact crosshead displacement caused the impact energy localized around the impacted area which leaded to fracture and penetration of that area for FML panels with plain weave composite fibre.

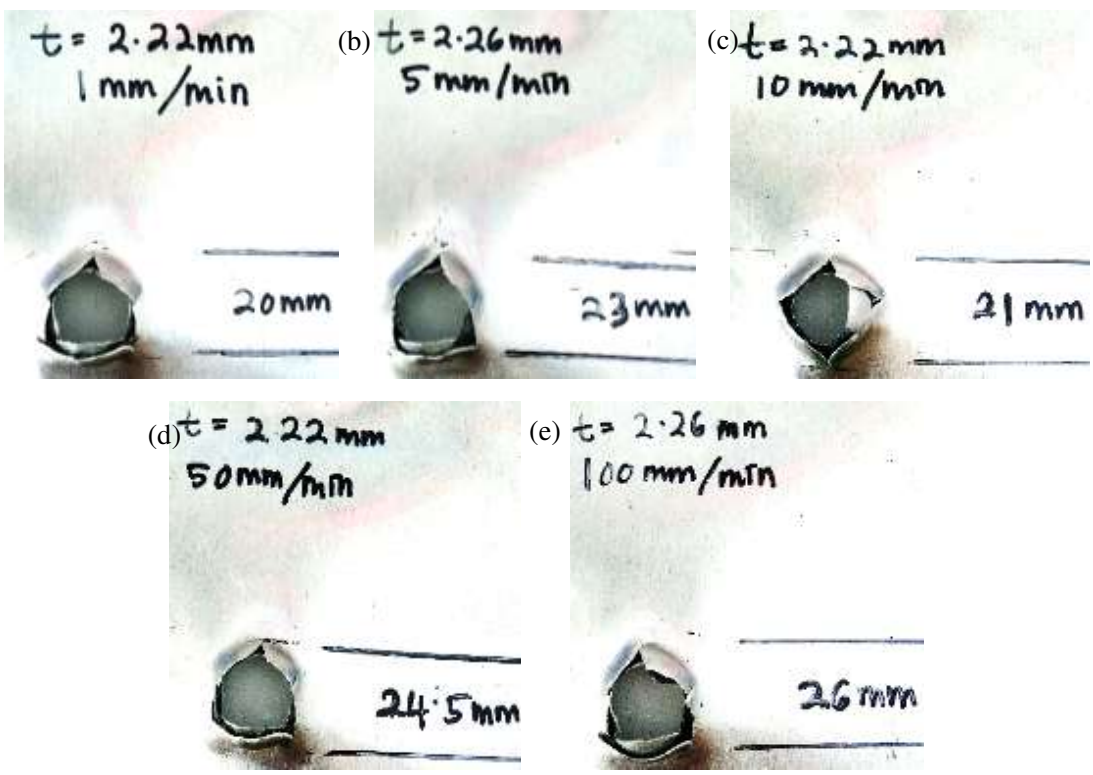

Figure 4. The visual result FML penetration based on different crosshead displacement.

The 2/1 FML model based on aluminium and carbon fibre was predicted through a finite element method; Abaqus. The numerical analysis was done as to predict the failure behavior of the FML model under the dynamic impact loading. The model was analysed by different velocities. The failure mechanism of the model was recorded. The FE model became successful when at the perforation stage of the impact event. The failure area of the FML increased because the impact velocity has been applied increasingly. The FML exhibited and appeared with little plastic deformation at the impact location. The plastic deformation was in aluminium and there was a fracture on the composite ply. The results clearly showed that the different impact velocity resulted in the flexural stiffness. The number of elements for indenter is 1345 while for the FML consisted with 4715 number of elements.

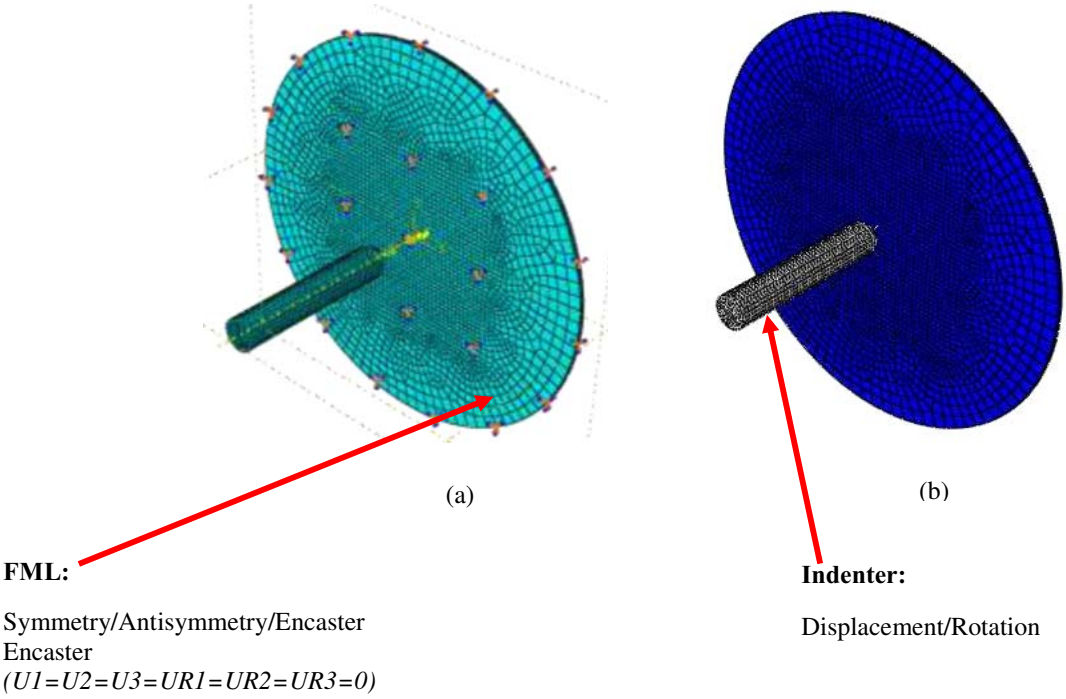

Figure 5. (a) Meshing and boundary condition of FML (b) simulation of FML.

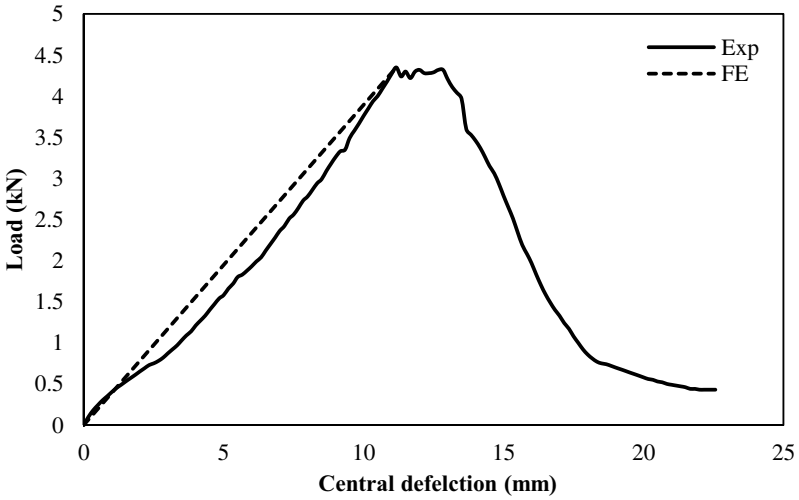

Figure 6. Validation graph between experimental and finite analysis data.

5. Conclusions

The experimental investigation was done and the finite element analysis of quasi-static test on 2/1 FMLs was presented in details. The bonding at interlayer of the FML was improved by metal sanding method. The impact area increased as the crosshead displacement was increased from 1 to 100 mm/min. The failure behaviour of the aluminium/CFRP laminate composite was modelled and analysed using finite element method, Abaqus/Explicit. As expected, the surface area from the impact loading increased when

the impact velocity also has been increased. The finite element analysis was successfully predicted in load-displacement for the hybrid laminates and identifying the failure behaviour of the hybrid laminate.

The prediction offered by the numerical model was found that the validation has good agreement with the experimental data which provide an appropriate value for the initial imperfection value was ran through the analysis. The analysis was based on the impact failure response of the fibre metal laminate by the quasi-static loading. According to the fact that the numerical model was assumed as a perfect bonding between the composite material and sheet metal since did not include the effect of initial imperfection along the fibre metal laminate.

A study to investigate the failure response of fibre metal laminate based various crosshead displacement and found that when the FML indented by higher crosshead displacement, the strength of the FML would also increase. Further work will investigate the behavior of the fibre metal laminate by using Abaqus/Explicit in order to capture the crushing behavior of the laminate.

On the basis results that have been obtained through the experimental work, the behaviors of the laminates were investigated through a load-displacement curve. The high value of maximum load stipulated to high resistance of the fibre metal laminates to the quasi-static indentation. The relationship between indentation crosshead displacements and the laminates thickness have been confirmed by the experimental research. The value of the maximum load that has been recorded by the aluminium/CFRP was about 4.11 kN.

The evaluation on the damaged fibre metal laminate it is possible to compare the damaged surface areas by an experimental research. It has been found that, increasing of crosshead displacement would increase the damage surface area. A detail observation on the cross-section of the fibre metal laminates were revealed by the presence of matrix cracking and delamination between composite layers as well as delamination at metal-composite interface.

The laminate thickness was lead to degradation degree. The lower thickness of laminates would have greater deformation and lower metal layer cracking. A laminate increased with thickness was accompanied by decreasing in degree of laminate deformation and occurring delamination between the individual composite layers and delamination on metal-composite interface.

Acknowledgments
The authors are grateful to the Ministry of Higher Education and Universiti Malaysia Pahang for funding this research RDU 1603108

References

[1] Vlot A, Krull M 1997 *J. Phys. IV* **7** C3-1045-C3-50.
[2] Chai G B, Manikandan P 2014 *Composite Structures* **107** 363-81.
[3] Nakatani H, Kosaka T, Osaka K, Sawada Y 2011 *Composites Part A: Applied Science and Manufacturing* **42** 772-81.
[4] Sarlin E, Apostol M, Lindroos M, Kuokkala V-T, Vuorinen J, Lepistö T, et al. 2014 *Compos. Struct.* **108** 886-93.
[5] Zhang Z, Wang W, Rans C, Benedictus R 2016 *Procedia Structural Integrity* **2** 3361-8.
[6] Pärnänen T, Kanerva M, Sarlin E, Saarela O 2015 *Composite Structures* **119** 777-86.
[7] Sadighi M, Alderliesten R C, Benedictus R 2012 *International Journal of Impact Engineering* **49** 77-90.
[8] Bieniaś J, Jakubczak P, Surowska B, Dragan K 2015 *Archives of Civil and Mechanical Engineering* **15** 925-32.
[9] Hu Y, Zheng X, Wang D, Zhang Z, Xie Y, Yao Z 2015 *J. Mater. Process. Technol.* **226** 32-9.

[10] Su Z, Ye L 2009 *Identification of damage using Lamb waves: from fundamentals to applications* (Springer Science & Business Media).
[11] Ghadami A, Behzad M, Mirdamadi H R 2015 *Archive of Applied Mechanics* **85** 793-804.
[12] Edson Cocchieri Botelho R A S, Luiz Cláudio Pardini, Mirabel Cerqueira Rezende 2006 Materials Research 9 247-56.
[13] Rezende M C, Botelho E C 2000 *Polímeros* **10** e4-e10.
[14] Zhang P, Ruan J, Li W 2001 *Cryogenics* **41** 245-51.
[15] Botelho E C, Nogueira C L, Rezende M C 2002 *J. Appl. Polym. Sci.* **86** 3114-9.
[16] Botelho E C, Scherbakoff N, Rezende M C, Kawamoto A M, Sciamareli J 2001 Macromolecules 34 3367-75.
[17] Bhatnagar N, Ramakrishnan N, Naik N, Komanduri R 1995 I*nternational Journal of Machine Tools and Manufacture* **35** 701-16.
[18] Potter K. *Introduction to composite products: design, development and manufacture: Springer Science & Business Media*; 1996.
[19] Gutowski T G P. Advanced composites manufacturing: John Wiley & Sons; 1997.
[20] Matthews F L, Rawlings R D 1999 *Composite materials: engineering and science* (Elsevier).
[21] Pardini L C, Peres R J 1996 *Polímeros* **6** 32-42.
[22] Hou M, Ye L, Lee H, Mai Y 1998 *Composites science and technology* **58** 181-90.
[23] Hillermeier R, Seferis J 2001 *Composites Part A: Applied Science and Manufacturing* **32** 721-9.
[24] Zenkert D 1997 *Student edition*.
[25] Rejab M, Cantwell W 2013 *Composites Part B: Engineering* **47** 267-77.
[26] Chang P Y, Yeh P C, Yang J M 2008 *Fatigue Fract. Eng. Mater. Struct.* **31** 989-1003.
[27] Chang P Y, Yeh P C and Yang J M 2008 *Mater. Sci. Eng., A* **496** 273-80.
[28] Vogelesang L and Vlot A 2000 *J. Mater. Process. Technol.* **103** 1-5.
[29] Li H, Hu Y, Fu X, Zheng X, Liu H and Tao J 2016 *Composite Structures* **152** 687-92.
[30] Botelho E C, Scherbakoff N and Rezende M C 2000 *Materials Research* **3** 19-23.
[31] Botelho E C, Scherbakoff N and Rezende M C 1999 *Polímeros: Ciência e Tecnologia* **1** 59-65.
[32] Lee C L and Wei K H 2000 *J. Appl. Polym. Sci.* **77** 2149-55.
[33] Phillips R, Glauser T and Månson J A E 1997 *Polymer composites* **18** 500-8.
[34] Shim S B, Seferis J C, Eom Y S and Shim Y T 1997 *Thermochimica Acta* **291** 73-9.
[35] Wingard C D 2000 *Thermochimica Acta* **357** 293-301.
[36] Hayes B, Gilbert E and Seferis J 2000 *Composites Part A: Applied Science and Manufacturing* **31** 717-25.
[37] Lee Y S, Wetzel E D and Wagner N J 2003 *J. Mater. Sci.* **38** 2825-33.
[38] Abrate S. Impact on composite structures: Cambridge university press; 2005.
[39] Richardson M and Wisheart M 1996 *Composites Part A: Applied Science and Manufacturing* **27** 1123-31.
[40] Katnam K, Da Silva L and Young T 2013 *Progress in Aerospace Sciences* **61** 26-42.
[41] Sinmazçelik T, Avcu E, Bora M Ö and Çoban O 2011 *Mater. Des.* **32** 3671-85.
[42] Morinière F D, Alderliesten R C and Benedictus R 2014 *International Journal of Impact Engineering* **67** 27-38.
[43] Liu G, Li Q, Msekh M A and Zuo Z 2016 *Comput. Mater. Sci.* **121** 35-47.
[44] Hashin Z 1980 *Journal of applied mechanics* **47** 329-34.
[45] Hashin Z and Rotem A 1973 *J. Compos. Mater.* **7** 448-64.
[46] Tsai S W and Wu E M 1971 *J. Compos. Mater.* **5** 58-80.
[47] Tsai S W. Strength Characteristics of Composite Materials. DTIC Document; 1965.
[48] Duarte A P C, Díaz Sáez A and Silvestre N 2017 *Thin-Walled Structures* **115** 277-88.